# A Silicon Balanced Subharmonic Optoelectronic Mixer for 60-GHz Fiber-Wireless Downlink Application

Minsu Ko, *Student Member, IEEE*, Jae-Young Kim, Myung-Jae Lee, *Student Member, IEEE*, Holger Rücker, and Woo-Young Choi, *Member, IEEE*

***Abstract*—We demonstrate a 60-GHz fiber-wireless downlink using a balanced subharmonic optoelectronic mixer based on a silicon avalanche photodiode (APD) pair fabricated with standard 0.25-$\mu$m bipolar complementary metal–oxide–semiconductor technology. Conversion efficiency of this new type of optoelectronic mixer is 11 dB better than that of the previously reported single APD mixer. We achieve downlink transmission of 25-Mb/s 32 quadrature-amplitude modulation data with the minimum error-vector magnitude of 2.4%.**

***Index Terms*—Avalanche photodiode (APD), silicon photonics, 60-GHz band, subharmonic optoelectronic mixer (SHOEM).**

## I. Introduction

SILICON-BASED 60-GHz wireless technologies have been actively developed and they are now commercially available for wireless personal area network and uncompressed high-definition video transmission applications [1]. Furthermore, standards for 60-GHz wireless local area network (WLAN) applications are presently discussed that can satisfy ever-increasing WLAN bandwidth demands [2].

With the wide deployment of 60-GHz wireless systems, fiber-wireless systems are expected to play an important role in which broadband data are distributed from a central office (CO) to remote antenna units (RAUs) via low-loss large-bandwidth optical fiber [3]. The fiber-wireless systems are particularly interesting for 60-GHz applications as the small wireless coverage of 60-GHz signals requires many RAUs due to high path loss, and the total implementation costs can be greatly reduced with the help of fiber.

We have previously demonstrated several types of subharmonic optoelectronic mixers (SHOEMs) [4]–[6]. In 60-GHz remote up-conversion fiber-wireless downlink, data carried over intermediate frequency (IF) are optically transmitted to RAU and up-converted to the 60-GHz band for wireless transmission, as shown in Fig. 1. Subharmonic local-oscillator (LO) signals, such as 30-GHz LO shown in the figure, are often used for cost reduction. The SHOEM in RAU can convert optical IF signals to electrical radio-frequency (RF) signals directly with multifunctionality of photodetection and frequency conversion. We are particularly interested in SHOEMs based on avalanche photodiodes (APDs) realized in silicon technologies [7] because this allows monolithic integration of SHOEMs with silicon millimeter-wave circuits providing the single-chip solution for RAU except the antenna. Although our investigations are based on APDs for 850-nm applications, high-performance 1550-nm APDs which can be integrated in silicon technology have been reported [8] and our approach can be easily extended to 1550-nm applications.

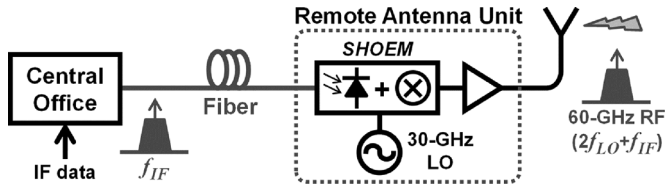


Fig. 1. Schematic diagram of 60-GHz fiber-wireless systems using SHOEM.

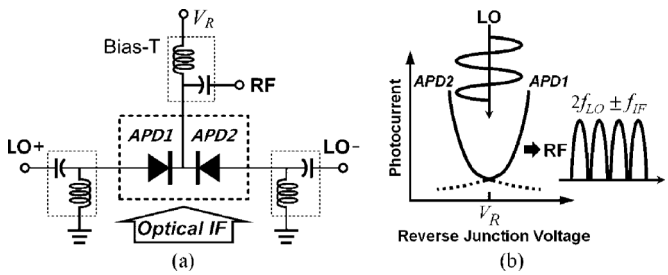


Fig. 2. (a) Schematic and (b) operation principle of the balanced SHOEM.

In this letter, we demonstrate a new type of silicon SHOEM based on a balanced APD pair. The balanced structure greatly improves frequency conversion efficiency and, consequently, reduces the LO power requirement to the level easily achieved with silicon technology. We verify the performance of our new SHOEM with 60-GHz fiber-wireless downlink demonstration.

## II. Balanced Subharmonic Optoelectronic Mixer

The schematic and the operation principle of the proposed balanced SHOEM are shown in Fig. 2. It is similar to singly balanced frequency doublers acting as full-wave rectifiers [9], [10] except that APDs with high reverse bias voltage, $V_R$, are used for photodetection and optoelectronic mixing. Optical IF signals

Manuscript received July 09, 2011; revised August 24, 2011; accepted September 14, 2011. Date of publication September 26, 2011; date of current version November 11, 2011. This work (2010-0014798) was supported by the Mid-career Researcher Program through an NRF grant funded by the MEST.

M. Ko, M.-J. Lee, and W.-Y. Choi are with the Department of Electrical and Electronic Engineering, Yonsei University, Seoul 120-749, Korea (e-mail: chrono9@yonsei.ac.kr; fodlmj@yonsei.ac.kr; wchoi@yonsei.ac.kr).

J.-Y. Kim was with the Department of Electrical and Electronic Engineering, Yonsei University, Seoul 120-749, Korea. He is now with NTT Microsystem Integration Laboratories, NTT Corporation, Atsugi, Kanagawa 243-0198, Japan (e-mail: kim.jaeyoung@lab.ntt.co.jp).

H. Rücker is with IHP, 15236 Frankfurt (Oder), Germany (e-mail: ruecker@ihp-microelectronics.com).

Digital Object Identifier 10.1109/LPT.2011.2169664

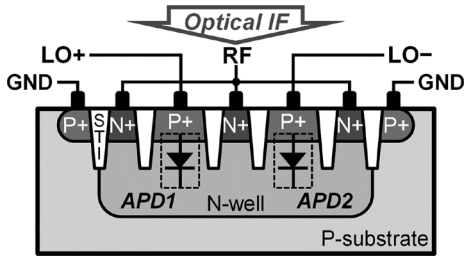


Fig. 3. Cross-section of the balanced SHOEM.

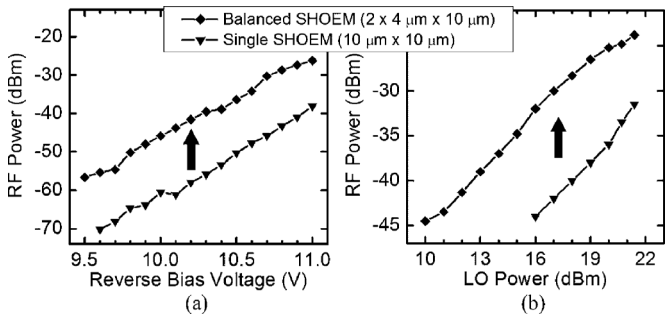


Fig. 4. Measured 60.1-GHz up-converted RF signal powers of balanced and single SHOEMs at (a) different reverse bias voltages with 19-dBm LO power and (b) different LO powers with 11.0-V reverse bias voltage.

injected into two APDs generate in-phase photocurrents. When LO signals are differentially applied to the APD anodes, they modulate avalanche gain of two APDs in the opposite direction. Since the APD pair acts as a full-wave rectifier for LO signals, a train of half-sinusoidal pulses consisting of even harmonics are produced, among which the second harmonic is dominant. The resulting photocurrents at the RF port then have the frequency component at $2f_{LO} \pm f_{IF}$. Because all the odd LO harmonics including the fundamental are rejected inherently, it requires no filtering of unwanted harmonics.

The balanced SHOEM was realized with complementary metal oxide semiconductor (CMOS) fabrication steps available within IHP's 0.25-$\mu$m SiGe:C bipolar CMOS technology [11]. Fig. 3 shows the cross-section of the SHOEM. Two P+ regions and shared N-well region form a pair of vertical PN-junction APDs both of which detect vertically incident 850-nm optical signals through a lensed fiber. Each APD has the lateral dimension of 4 $\mu$m$\times$ 10 $\mu$m, and they are separated by 2 $\mu$m. The overall dimension of optical window is 10 $\mu$m$\times$ 10 $\mu$m. Shrinking the diode size is very important to reduce the diode junction capacitance for better photodetection and mixing efficiencies [6]. In our case, the shrink is limited by the spot diameter of a lensed fiber.

Performance enhancement of the balanced SHOEM is verified with the 10 $\mu$m$\times$ 10 $\mu$m single SHOEM having the same layer structure. Fig. 4(a) and (b) show measured 60.1-GHz up-converted RF signal powers of two SHOEMs at different reverse bias voltages and 30-GHz LO powers, respectively. For these measurements, 0-dBm 100-MHz optical IF signals were used. As can be seen in the figure, the balanced SHOEM has 11-dB conversion efficiency improvement over the wide range of bias voltages and LO powers. This improvement is due to more efficient LO driving capability in the balanced structure as well as reduced capacitance provided by smaller

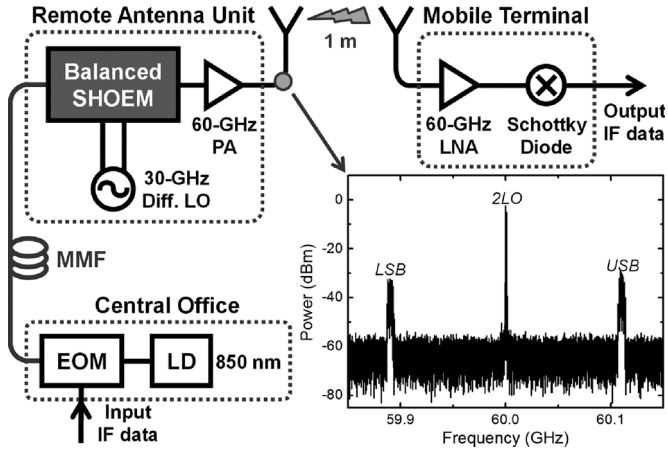


Fig. 5. Experimental setup for 60-GHz fiber-wireless downlink based on double-sideband self-heterodyne wireless transmission. The inset shows measured power spectrum of transmitted signals at RAU.

APD dimensions. Details of device analysis with equivalent circuit models are given in [12].

## III. 60-GHz Fiber-Wireless Downlink Demonstration

60-GHz fiber-wireless downlink transmission is demonstrated using the balanced SHOEM. Fig. 5 shows the experimental setup based on double-sideband self-heterodyne wireless transmission [13]. In CO, an electrooptic modulator (EOM) modulates 850-nm light with 25-Mb/s 32 quadrature-amplitude modulation (QAM) data at 110-MHz carrier generated by Agilent E4432B signal generator. Although the photodetection bandwidth of the APD used for SHOEM is about 5 GHz, relatively small optical IF of 110 MHz is used. This is because there is impedance mismatch between the SHOEM output port and the 60-GHz power amplifier (PA) input port, which can reduce power delivery efficiency for broadband signals. This problem can be solved by adding integrated circuits for impedance matching at the SHOEM.

The modulated optical signals are transmitted to RAU through 4-m-long multimode fiber (MMF). In RAU, transmitted signals are injected into the SHOEM. 30-GHz differential LO signals generated by a signal generator with a 180° hybrid are also applied to the SHOEM in an on-wafer probing setup. 60-GHz up-converted RF signals are amplified by a PA having 27.5-dB gain and radiated to mobile terminals using a 24-dBi horn antenna. The inset of Fig. 5 shows the measured power spectrum of transmitted signals at RAU. Lower-sideband (LSB) and upper-sideband (USB) signals at 59.89 and 60.11 GHz, respectively, are shown in the spectrum. After 1-m wireless transmission, the signals are received by another horn antenna and amplified by a low-noise amplifier (LNA) having 18.3-dB gain and 4.8-dB noise figure. Then, they are detected by a Schottky diode. This self-heterodyne scheme is used instead of more efficient super-heterodyne scheme for its simplicity.

Error-vector magnitude (EVM) and signal-to-noise ratio (SNR) performances of recovered data at the output of the mobile terminal are analyzed with Agilent 89600 vector signal analyzer. The measured minimum EVM and SNR are 2.4% and 28.6 dB at 11.1-V APD bias, 12-dBm LO, and 0-dBm optical IF. Constellation and power spectrum of output data at

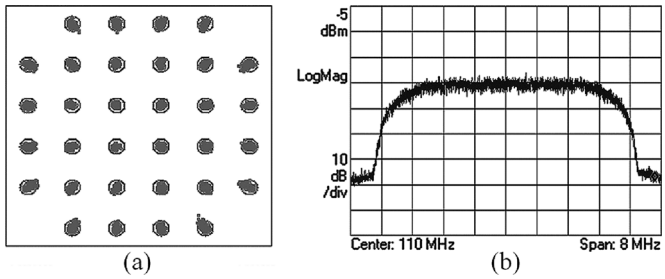


Fig. 6. (a) Constellation and (b) power spectrum of 110-MHz-carrier 25-Mb/s 32QAM output IF data. The reverse bias voltage of 11.1 V, the LO power of 12 dBm, and the optical IF power of 0 dBm are applied to the SHOEM.

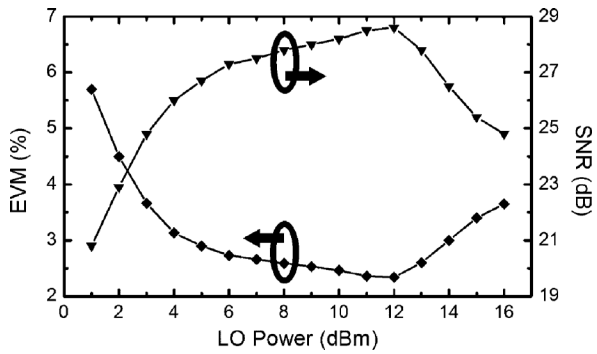


Fig. 7. EVM and SNR versus LO power at 0-dBm optical IF power.

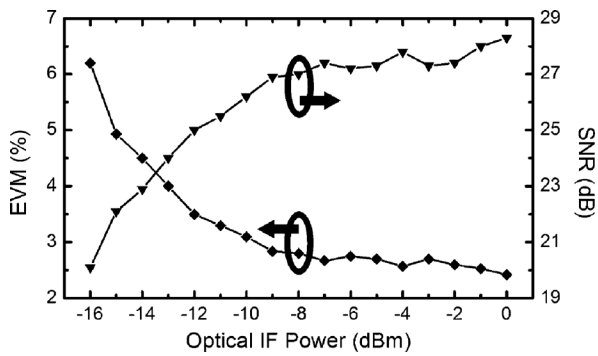


Fig. 8. EVM and SNR versus optical IF power at 12-dBm LO power.

this condition are shown in Fig. 6. The results indicate 2.7% enhancement in EVM with 8-dB lower LO power, compared to the link using the single SHOEM reported in [4].

Fig. 7 shows EVM and SNR versus LO powers. Increasing LO power enhances frequency conversion efficiency of the SHOEM and improves EVM and SNR because the link noise is dominated by avalanche photodetection in the SHOEM and not influenced by LO power. With LO power over 12 dBm, however, EVM and SNR begin to degrade. This is caused by increase in currents with higher LO power which shifts the bias voltage away from the optimal value. The results show that LO power can be reduced to 2 dBm for 5% EVM, which is a reasonable requirement for many applications. For example, 64QAM modulation specified in 60-GHz WLAN standardization requires 5.6% EVM [2]. Such LO powers can be achieved with silicon integrated 30-GHz oscillators [14].

EVM and SNR versus optical IF power are shown in Fig. 8. The link performance degrades as optical IF power decreases because the output SNR of the SHOEM is reduced. However, improvement in EVM and SNR with increasing optical IF power saturates at about −10-dBm optical IF power. This is due to the nonlinearities in the link caused by the EOM. For 5% EVM, optical input sensitivity is about −15 dBm. With this sensitivity, this scheme can be used up to several kilometers of MMF having, for example, attenuation of 2.3 dB/km and effective modal bandwidth of 4700 MHz · km as is the case for Corning ClearCurve multimode fiber.

## IV. Conclusion

We introduce a new type of SHOEM based on a balanced silicon APD pair and successfully demonstrate cost-effective 60-GHz fiber-wireless downlink using the new device. The balanced SHOEM provides much better conversion efficiency resulting in much better link performance compared to previously reported results. We believe our balanced SHOEM can find useful applications in realizing low-cost integrated RAU for 60-GHz fiber-wireless systems.

## Acknowledgment

The authors would like to thank IDEC for EDA software support.

## References

[1] A. M. Niknejad, "Siliconization of 60 GHz," *IEEE Microw. Mag.*, vol. 11, pp. 78–85, Feb. 2010.
[2] *Task Group*, IEEE 802.11ad.
[3] H. Ogawa, D. Polifko, and S. Banba, "Millimeter-wave fiber optics systems for personal radio communication," *IEEE Trans. Microw. Theory Tech.*, vol. 40, no. 12, pp. 2285–2293, Dec. 1992.
[4] H.-S. Kang and W.-Y. Choi, "Fibre-supported 60 GHz self-heterodyne systems based on CMOS-compatible harmonic optoelectronic mixers," *Electron. Lett.*, vol. 43, no. 20, pp. 1101–1103, Sep. 2007.
[5] M. J. Lee, H. S. Kang, K. H. Lee, and W. Y. Choi, "Self-oscillating harmonic opto-electronic mixer based on a CMOS-compatible avalanche photodetector for fiber-fed 60-GHz self-heterodyne systems," *IEEE Trans. Microw. Theory Tech.*, vol. 56, no. 12, pt. 2, pp. 3180–3187, Dec. 2008.
[6] J.-Y. Kim, M.-J. Lee, and W.-Y. Choi, "60 GHz CMOS-APD optoelectronic mixers with optimized conversion efficiency," in *Proc. IEEE Int. Topical Meeting Microw. Photon.*, Montreal, Canada, 2010, pp. 139–142.
[7] H.-S. Kang, M.-J. Lee, and W.-Y. Choi, "Si avalanche photodetectors fabricated in standard complementary metal-oxide-semiconductor process," *Appl. Phys. Lett.*, vol. 90, pp. 151118-1–151118-3, Apr. 2007.
[8] S. Assefa, F. Xia, and Y. A. Vlasov, "Reinventing germanium avalanche photodetector for nanophotonic on-chip optical interconnects," *Nature*, vol. 464, no. 7285, pp. 80–84, Mar. 2010.
[9] S. A. Maas, "Diode frequency multipliers," in *Nonlinear Microwave and RF Circuits*, 2nd ed. Norwood, MA: Artech House, ch. 7, pp. 355–393.
[10] B. Mayer and R. Knoechel, "Biasable balanced mixers and frequency doublers using a new planar balun," in *Proc. 20th Eur. Microw. Conf.*, 1990, pp. 1027–1032.
[11] B. Heinemann, R. Barth, D. Knoll, H. Rücker, B. Tillack, and W. Winkler, "High-performance BiCMOS technologies without epitaxially-buried subcollectors and deep trenches," *Semicond. Sci. Technol.*, vol. 22, no. 1, pp. S153–S157, Jan. 2007.
[12] J.-Y. Kim, M. Ko, M.-J. Lee, H. Rücker, and W.-Y. Choi, "60-GHz-band subharmonic optoelectronic mixer based on CMOS avalanche photodiode pair," *IEEE Trans. Microw. Theory Tech.*, submitted for publication.
[13] Y. Shoji, K. Hamaguchi, and H. Ogawa, "A low-cost and stable millimeter-wave transmission system using a transmission-filter-less double-side-band millimeter-wave self-heterodyne transmission technique," *IEICE Trans. Commun.*, vol. E86-B, no. 6, pp. 1884–1892, Jun. 2003.
[14] A. Parsa and B. Razavi, "A new transceiver architecture for the 60-GHz band," *IEEE J. Solid-State Circuits*, vol. 44, no. 3, pp. 751–762, Mar. 2009.